Max-Planck-Institut
für Mathematik
in den Naturwissenschaften
Leipzig

Geometric singular perturbation analysis of an autocatalator model

by

Ilona Gucwa, and Peter Szmolyan

Preprint no.: 43 2009

GEOMETRIC SINGULAR PERTURBATION ANALYSIS OF AN AUTOCATALATOR MODEL

I. GUCWA AND P. SZMOLYAN

ABSTRACT. A singularly perturbed planar system of differential equations modeling an autocatalytic chemical reaction is studied. For certain parameter values a limit cycle exists. Geometric singular perturbation theory is used to prove the existence of this limit cycle. A central tool in the analysis is the blow-up method which allows the identification of a complicated singular cycle which is shown to persist.

1. Introduction

We consider the planar system of differential equations

$$\begin{aligned} \dot{a} &= \mu - a - ab^2, \\ \varepsilon \dot{b} &= -b + a + ab^2, \end{aligned} \tag{1.1}$$

where $(a, b) \in \mathbb{R}^2$, $\mu \in \mathbb{R}$ and the parameter $\varepsilon > 0$ varies in a small interval around zero. System (1.1) is a model for an autocatalytic chemical process with the variables a and b being scaled concentrations. The autocatalytic nature of the process is modeled by the ab^2 term, i.e. the production rate of b increases linearly with the concentration of b, see e.g. [20], [22]. Naturally the physically meaningful range of the variables is $a, b \geq 0$. Our main result is that for $\mu > 1$ and ε sufficiently small system (1.1) has a globally attracting limit cycle of relaxation type.

Due to the occurrence of the small parameter ε solutions evolve on several time scales. System (1.1) is written in the standard form of slow-fast systems with the slow variable a and the fast variable b. The derivative in (1.1) is with respect to slow time scale t. By transforming to the fast variable $\tau := t/\varepsilon$ we obtain the equivalent fast system

$$\begin{aligned} a' &= \varepsilon(\mu - a - ab^2), \\ b' &= -b + a + ab^2, \end{aligned} \tag{1.2}$$

where $'$ denotes differentiation with respect to τ. Setting $\varepsilon = 0$ defines two limiting systems: *the reduced system* (obtained from (1.1))

$$\begin{aligned} \dot{a} &= \mu - a - ab^2, \\ 0 &= -b + a + ab^2, \end{aligned} \tag{1.3}$$

and *the layer problem* (obtained from (1.2))

$$\begin{aligned} a' &= 0, \\ b' &= -b + a + ab^2. \end{aligned} \tag{1.4}$$

1991 *Mathematics Subject Classification.* Primary: 34C26, 34C30, 34C40, 34E15, 34E20, 37C10, 37C27.

Key words and phrases. slow-fast system, geometric singular perturbation theory, slow manifolds, blow-up, relaxation oscillations.

The research of the first author was supported by the Austrian Science Foundation under grant W8 and the International Max Planck Research School Mathematics in the Sciences in Leipzig.

The research of the second author was supported by the Austrian Science Foundation under grant W8 and grant Y 42-MAT.

In problems of this type the reduced problem captures essentially the slow dynamics and the layer problem captures the fast dynamics. The layer problem is a one dimensional dynamical system in the fast variable b with the slow variable a acting as a parameter. The equation

$$-b + a + ab^2 = 0 \tag{1.5}$$

defines the *critical manifold* S of the steady states of the layer problem, see Figure 1. The reduced problem describes the dynamics on the critical manifold S.

Due to results by Fenichel [7], normally hyperbolic pieces of critical manifolds perturb smoothly to locally invariant *slow manifolds* for ε sufficiently small. Hence, under suitable assumptions orbits of a singularly perturbed system can be obtained as perturbations of singular orbits consisting of pieces of orbits of the reduced problem and of the layer problem, see [11] for more details and applications.

A prototypical example for this procedure is the construction of relaxation cycles of the well-known Van der Pol oscillator [8], [19]. The *fold points* of the critical manifold have been a substantial difficulty in the analysis of Van der Pol-type relaxation oscillations. At fold points and other points where normal hyperbolicity of the critical manifold is lost, the existence of slow manifolds under ε-perturbations is not guaranteed. The blow-up method pioneered by Dumortier and Roussarie [4] has proven to be a powerful tool in the geometric analysis of such problems [2], [5], [6], [10], [12], [13], [14], [15], [21].

In our analysis of system (1.1) we will encounter a fold point but also other non-hyperbolic points which will be treated by suitable blow-ups. We will show that for $\mu > 1$ and ε sufficiently small system (1.1) has a globally attracting limit cycle of relaxation type. However, the asymptotic behavior and the global structure of the limit cycle is considerably more complicated than that for the Van der Pol oscillator. It will turn out that additional scalings are needed to capture the full dynamics since for $b = O(1/\varepsilon)$ the dynamics and limiting behavior are not captured by problems (1.3) and (1.4). In the regime $b = O(1/\varepsilon)$ the cubic terms in system (1.1) dominate and a different slow-fast structure emerges. Thus, it is necessary to match the regime $b = O(1)$ with the regime $b = O(1/\varepsilon)$. We will demonstrate that the blow-up method is a convenient tool for geometric matching of these two regimes. It will turn out that several iterated blow-ups have to be used to obtain a complete desingularization of the problem. In fact, this novel feature motivated much of our interest in the problem.

On the other hand the basic blow-up analysis in Section 3 is rather straightforward and algebraically simple. Hence, we feel that the geometric analysis of the Autocatalator problem could serve as an introduction to the area of geometric desingularization of slow-fast systems in the context of an specific example. For another introduction to the method in the context of singularly perturbed planar fold points we refer to [13].

The complicated dynamics of a related three-dimensional system, where roughly speaking μ becomes a dynamic variable, has been studied numerically and analytically in [16], [17], [18], [20]. The main feature of that system is the occurrence of mixed-mode oscillations which consist of periodic or chaotic sequences of small and large oscillations. Mixed-mode oscillations have been related to certain types of canards, which generate the small oscillations while the large oscillations are often of relaxation type [2], [12], [16], [17], [18]. In [17] a mechanism for the occurring large relaxation oscillations was proposed. Here, we will give a detailed analysis of this mechanism in the context of the planar system (1.1).

The article is organized as follows. In Section 2 we analyze the dynamics and asymptotic behavior of the autocatalator in the regimes $b = O(1)$ and $b = O(1/\varepsilon)$. Section 3 presents the blow-up analysis. In Section 4 we prove the existence of a periodic orbit of relaxation type for the blown-up system. Section 5 contains some remarks about canard cycles of system (1.1) which occur for $\mu \approx 1$. In order not to interrupt the main argument and to avoid confusing notation the proof of Theorem 4.4 based on a second blow-up procedure is given in Appendix A.

2. Slow–fast analysis of the autocatalator

2.1. **Regime 1: $b = O(1)$.** We begin by discussing some of the basic properties of the layer problem (1.4) and the reduced problem (1.3). The layer problem is a one dimensional dynamical system in the fast variable b with the slow variable a acting as a parameter. The critical manifold S

$$S = \{(a,b): \quad a - b + ab^2 = 0\} \tag{2.1}$$

is the manifold of steady states of the layer problem. S is a graph $a = \frac{b}{1+b^2}, b \geq 0$, (see Figure 1). The linearized stability of points in S as the steady states of the

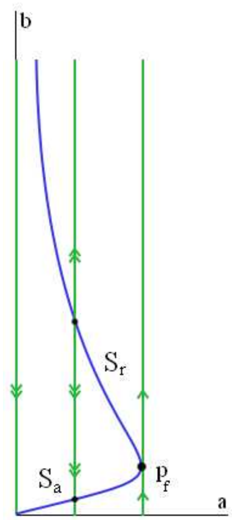

Figure 1. Critical manifold S and fast flow of the layer problem (1.4).

layer problem (1.4) is determined by the sign of $\frac{b^2-1}{1+b^2}$, thus the manifold S consists of an attracting branch S_a with $b < 1$, a repelling branch S_r with $b > 1$, and a non-hyperbolic fold point $p_f = (1/2, 1)$.

The slow dynamics of the reduced problem (1.3) on the critical manifold S is obtained by differentiating equation $a = \frac{b}{1+b^2}$ with respect to time t and substituting this expression into $\dot{a} = \mu - a - ab^2$, which gives

$$\dot{b} = \frac{1+b^2}{1-b^2}(\mu - b). \tag{2.2}$$

This system is singular at $b = 1$ and has a steady state for $b = \mu$. Three different cases can be distinguished (depicted in Figure 2):

(1) For $\mu < 1$ the steady state is stable and lies on the attracting critical manifold S_a. All solutions corresponding to $b > \mu$ approach the fold in finite backward time.
(2) For $\mu = 1$ there is no equilibrium since the singularity in (2.2) at $b = 1$ cancels and the reduced flow passes through the fold point.

(3) For $\mu > 1$ the steady state is unstable and lies on the repelling manifold S_r. All solutions corresponding to $b < \mu$ approach the fold in finite forward time.

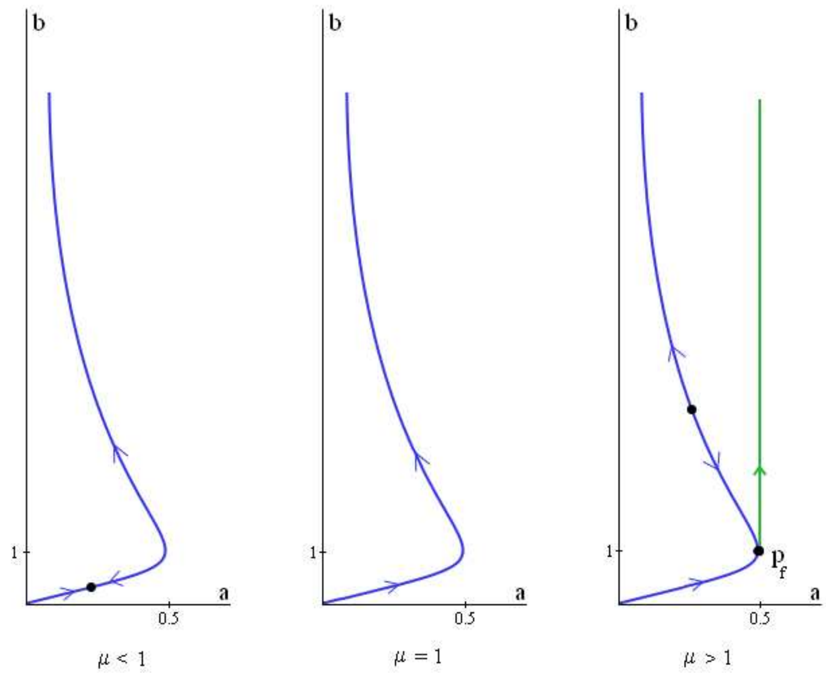

FIGURE 2. Dynamics of the reduced problem (2.2) depending on parameter μ.

In this work we focus on the case $\mu > 1$. In the singular limit solutions starting on the left side of S are rapidly attracted to S_a, follow the reduced dynamics until they reach the fold point and then jump up vertically along the orbit $a = \frac{1}{2}$ of the layer problem. Thus, we have the familiar phenomenon of a jump point in Regime 1, see the $\mu > 1$ case in Figure 2.

A precise description of the dynamics for $0 < \varepsilon << 1$ can be given by combining standard Fenichel theory [7] with the blow-up analysis of planar fold points given in [13]. We conclude from [7] that outside a small neighborhood of the fold point p_f, the manifolds S_a and S_r persist as nearby invariant slow manifolds $S_{a,\varepsilon}$, $S_{r,\varepsilon}$, respectively for ε small, i.e.

Theorem 2.1. *For small $\delta > 0$ there exist $\varepsilon_0 > 0$ and smooth functions $b = h_{a,\varepsilon}(a)$ and $b = h_{r,\varepsilon}(a)$ defined on $I_a := [-\delta, \frac{1}{2} - \delta]$ and $I_r := [\delta, \frac{1}{2} - \delta]$, respectively, such that the graphs*

$$S_{a,\varepsilon} = \{(a,b) : b = h_{a,\varepsilon}(a), a \in I_a\}, \qquad S_{r,\varepsilon} = \{(a,b) : b = h_{r,\varepsilon}(a), a \in I_r\}$$

are locally invariant attracting, respectively repelling slow manifolds of system (1.1) for $\varepsilon \in (0, \varepsilon_0]$.

At the fold point p_f where normal hyperbolicity fails, Fenichel theory does not apply. Nevertheless, the description of the dynamics near p_f for $\varepsilon \neq 0$ by using blow-up techniques has been given in [4], [13]. In particular, the asymptotic behavior of the continuation of $S_{a,\varepsilon}$ beyond the fold point has been studied in [13], see Section

4.1 for details. Hence, the singular limit behavior described above persists for small ε, i.e. all orbits starting between $S_{a,\varepsilon}$ and $S_{r,\varepsilon}$ are rapidly attracted by $S_{a,\varepsilon}$, follow the slow flow to the right and jump almost vertically to large values of b after passing the fold point, see Sections 4.5 and 4.1 for a detailed description based on suitably defined transition maps.

This analysis implies that for $\mu > 1$ limit cycles with $b = O(1)$ do not exist. In order to find a cycle for system (1.1) larger values of b must be taken into account.

2.2. **Regime 2:** $b = O(1/\varepsilon)$**.** For large values of b the cubic terms in (1.1) become dominant and the asymptotic behavior is not correctly described by the layer equations (1.4), i.e. new scales arise and a different asymptotic analysis is needed. This is best seen if the variables are rescaled according to

$$a = A, \qquad b = \frac{B}{\varepsilon}, \qquad T = t/\varepsilon^2. \tag{2.3}$$

In these variables the equations have the form

$$\begin{array}{rcl} A' &=& \mu\varepsilon^2 - A\varepsilon^2 - AB^2, \\ B' &=& -B\varepsilon + A\varepsilon^2 + AB^2, \end{array} \tag{2.4}$$

where $'$ denotes differentiation with respect to T.
Setting $\varepsilon = 0$ in (2.4) gives

$$\begin{array}{rcl} A' &=& -AB^2, \\ B' &=& AB^2. \end{array} \tag{2.5}$$

The A-axis and B-axis are two lines of equilibria, denoted by l_A and l_B, respectively, which intersect at the origin. Hence, system (2.4) is a singularly perturbed system which, however, is not in standard form since both variables evolve in the $\varepsilon = 0$ problem. Therefore, system (2.5) will be also called layer problem in the following.

The dynamics of this layer problem is rather simple, see Figure 3. The two lines of equilibria are connected by heteroclinic orbits, i.e. an equilibrium $(A_0, 0) \in l_A$ is connected to the equilibrium $(0, A_0) \in l_B$ by an orbit of the layer problem lying on the straight line $B = A_0 - A$. Outside of a neighborhood of the origin the line

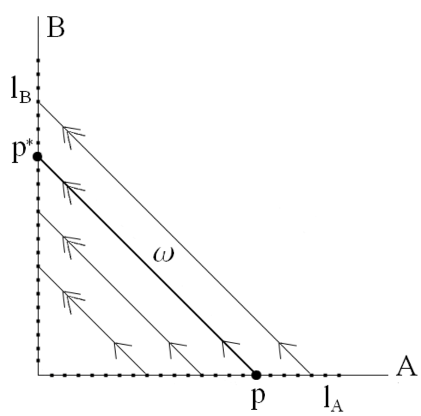

FIGURE 3. Dynamics of the layer problem (2.5).

l_B is exponentially attracting, whereas the line l_A is non-hyperbolic for the layer problem. Thus, any compact subset of the line l_B that does not contain the origin can be taken as a normally hyperbolic critical manifold M_0. Then, Fenichel theory

[7] implies the existence of a slow manifold M_ε that is a perturbation of M_0, i.e. lies within $O(\varepsilon)$ of M_0. More precisely, we have the following result.

Theorem 2.2. *Let $M_0 = \{(0,B) : B \in [B_0, B_1], B_0 > 0\}$. There exists $\varepsilon_0 > 0$ such that for $\varepsilon \in (0, \varepsilon_0]$ there exists a smooth locally invariant attracting one-dimensional slow manifold M_ε given as a graph*

$$M_\varepsilon = \{(A,B) : \ A = h(B,\varepsilon), B \in [B_0, B_1]\}. \tag{2.6}$$

The function $h(B,\varepsilon)$ is smooth and has the expansion $h(B,\varepsilon) = \varepsilon^2 \frac{\mu}{B^2} + O(\varepsilon^3)$.

Proof. The existence of the slow manifold as a graph $A = h(B,\varepsilon)$ follows from Fenichel Theory due to the normal hyperbolicity of M_0. By plugging the expansion of h in powers of ε into (2.4) and comparing coefficients of powers of ε the expansion (2.6) is easily obtained. □

The equation governing the slow dynamics on M_ε is found by substituting the function $h(B,\varepsilon)$ into (2.4). Hence, the slow flow on M_ε is governed by the equation

$$\frac{dB}{d\tau} = -B + O(\varepsilon), \tag{2.7}$$

where $\tau = \varepsilon T = t/\varepsilon$. We conclude that B decays exponentially on M_ε.

Thus, Regime 2 provides the following mechanism for obtaining a closed singular cycle. All of Regime 1 is compressed into the non-hyperbolic line of equilibria l_A. In particular, the fold point p_f of the critical manifold S and its fast fiber in Regime 1 collapse into the point $p = (1/2, 0)$. The point p is connected to the point $p^* = (0, 1/2) \in l_B$ by a heteroclinic orbit ω of the layer problem (2.5). From there the singular orbit follows the reduced dynamics (2.7) along the critical manifold M_0 until it reaches the origin. Thus, we introduce the singular cycle $\gamma_0 := S_A \cup \omega \cup S_B$, where S_A is the segment from the origin to p_f on l_A and S_B is the segment from p^* to the origin on l_B.

Note, however, that we have no valid description of the dynamics and asymptotics near the non-hyperbolic line l_A in Regime 2. A full description of the dynamics will be obtained by matching Regime 2 with Regime 1. In fact, we will prove the following theorem

Theorem 2.3. *For $\mu > 1$ and ε sufficiently small there exists a unique attracting periodic orbit γ_ε of system (2.4) and hence of the equivalent system (1.1) which tends to the singular cycle γ_0 for $\varepsilon \to 0$.*

We illustrate these results with numerical simulations obtained by using Mathematica 6. Figure 4 shows the limit cycle γ_ε for $\varepsilon = 0.001$ and $\mu = 3$ lying close to the singular cycle γ_0. In Figure 5 the part of γ_ε corresponding to Regime 1 is shown. The solution corresponding to the limit cycle is attracted to the slow manifold, follows the slow manifold and jumps to large values of b after passing the fold point. The unstable equilibrium is shown in Figure 5. Due to the scaling the unstable equilibrium seems to lie on the limit cycle in Figure 4.

The matching of Regime 1 with Regime 2 will be done in a geometric way based on the blow-up technique. In the next section, we begin this blow-up analysis by defining a suitable blow-up of the non-hyperbolic line of steady states l_A. We analyze the dynamics of the blown-up system and define a better resolved singular cycle. In Section 4 we prove that the singular cycle of the blown-up system persists for $\varepsilon \neq 0$.

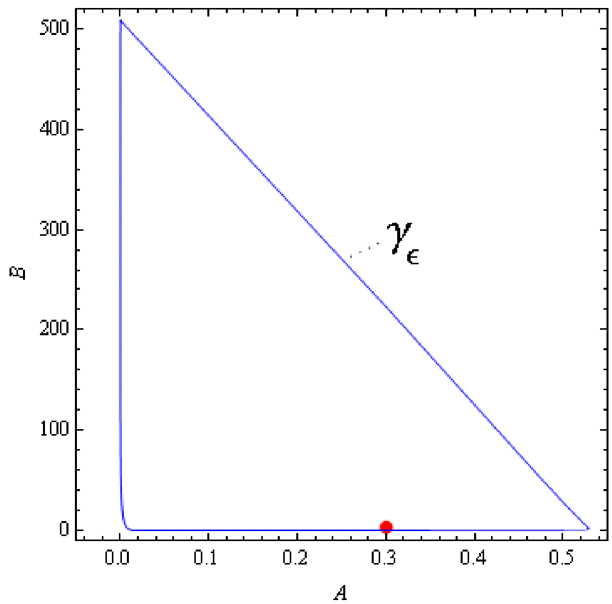

FIGURE 4. Limit cycle γ_ε for $\varepsilon = 0.001$ and $\mu = 3$ of system (2.4).

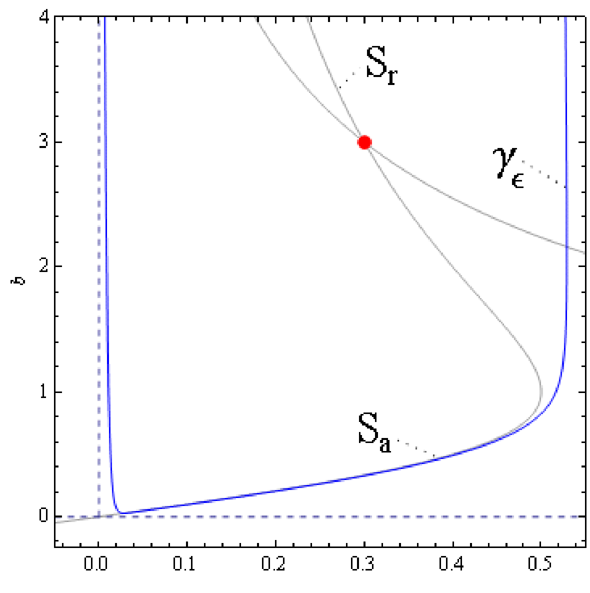

FIGURE 5. Part of the limit cycle γ_ε for $\varepsilon = 0.001$ and $\mu = 3$ in Regime 1.

3. Blow-up analysis

The starting point of our geometric analysis is the rescaled extended system in the form

$$\begin{aligned} A' &= \mu\varepsilon^2 - A\varepsilon^2 - AB^2, \\ B' &= -\varepsilon B + A\varepsilon^2 + AB^2, \\ \varepsilon' &= 0. \end{aligned} \tag{3.1}$$

System (3.1) is viewed as a three dimensional vector field X, i.e. ε is viewed as a variable instead of as a parameter. Note that the planes $\varepsilon = const.$ are invariant for this three dimensional system. In particular, on the plane $\varepsilon = 0$ the flow is given by the layer problem (2.5). Moreover, $l_A \cup \{0\}$ is a manifold of equilibria for (3.1) and the eigenvalues of the linearization of system (3.1) evaluated at these equilibria are all equal to zero. To overcome this degeneracy we apply the following blow-up transformation

$$A = \bar{a}, \quad B = r\bar{b}, \quad \varepsilon = r\bar{\varepsilon}. \tag{3.2}$$

with $\bar{a} \in \mathbb{R}$, $(\bar{b}, \bar{\varepsilon}) \in \mathbb{S}^1 = \{(\bar{b}, \bar{\varepsilon}) | \ \bar{b}^2 + \bar{\varepsilon}^2 = 1\}$, and $r \in \mathbb{R}_0^+$. The blow-up transformation simply introduces polar coordinates in the (B, ε)-plane. For $r > 0$ the blow-up transformation is a diffeomorphism. The preimage of the singular line $l_A \times \{0\}$ is the cylinder $Z = \mathbb{R} \times \mathbb{S}^1 \times \{0\}$, i.e. the singular line $l_A \times \{0\}$ is blown-up to the cylinder Z, see Figure 6.

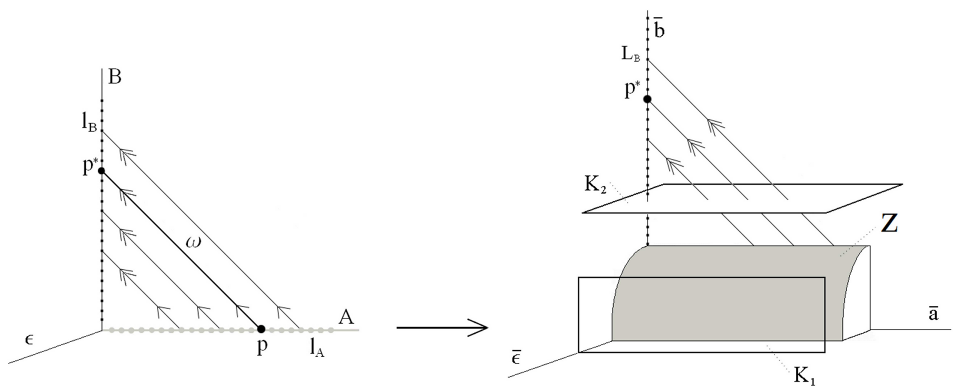

FIGURE 6. Blow-up transformation (3.2) for system (3.1) and local charts K_1 and K_2.

The vector field (3.1) induces a vector field $\bar{X}$ on the blown-up space $\mathbb{R} \times \mathbb{S}^1 \times \mathbb{R}_0^+$. Since the cylinder Z is constructed as the blow-up of a line of equilibria, the blown-up vector field vanishes on the cylinder. To obtain a non-trivial flow on the cylinder the blown-up vector field must be desingularized by dividing out a factor r.

The blown-up vector field is analyzed in charts K_1 and K_2 defined by setting $\bar{\varepsilon} = 1$ and $\bar{b} = 1$, respectively, in the blow-up transformation (3.2). Thus, chart K_1 covers the front side of the cylinder corresponding to $\bar{\varepsilon} > 0$, while K_2 covers the upper part of the cylinder corresponding to $\bar{b} > 0$, see Figure 6. It turns out that after desingularization the blown-up vector field written in chart K_1 is precisely the original system (1.2). Thus the specific form of the blow-up transformation is directly linked to the form of the rescaling (2.3), see also Remark 3.2 below.

Remark 3.1. *Intuitively, it is clear that chart K_1 covers Regime 1 and that chart K_2 covers Regime 2. Note however, that a rigorous perturbation analysis in Regime 1 is only possible for bounded values of b whereas a rigorous perturbation analysis in Regime 2 is only possible for B bounded away from zero. It is an important property of the blow-up method that these results are recovered in the corresponding charts. In addition, the blow-up method provides a compactification of the region corresponding to unbounded b in Regime 1 and a desingularization of the nonhyperbolic line l_A in Regime 2 which allows to match the two regimes.*

3.1. **Dynamics in charts.** Consider the charts K_1 and K_2 defined by setting $\bar{\varepsilon} = 1$ and $\bar{b} = 1$ respectively, in the blow-up transformation (3.2). Hence, the blow-up transformation in charts K_i, $i = 1, 2$, is given by

$$A = a_1, \quad B = r_1 b_1, \quad \varepsilon = r_1, \tag{3.3}$$

$$A = a_2, \quad B = r_2, \quad \varepsilon = r_2 \varepsilon_2. \tag{3.4}$$

The change of coordinates κ_{12} from K_1 to K_2 is given by

$$a_2 = a_1, \qquad r_2 = r_1 b_1, \qquad \varepsilon_2 = 1/b_1. \tag{3.5}$$

We denote the inverse transformation of κ_{12} by κ_{21}.

Dynamics in chart K_1. By inserting (3.3) into system (3.1), we obtain the blown-up system, which is a family of planar vector fields with parameter r_1, (since $r_1' = 0$)

$$\begin{array}{lcl} a_1' & = & r_1^2(\mu - a_1 - a_1 b_1^2), \\ r_1 b_1' & = & r_1^2(a_1 b_1^2 + a_1 - b_1), \\ r_1' & = & 0. \end{array} \tag{3.6}$$

Now we desingularize the equations by rescaling time $t_1 := r_1 t$, so that the factor r_1 disappears. We obtain

$$\begin{array}{lcl} a_1' & = & r_1(\mu - a_1 - a_1 b_1^2), \\ b_1' & = & a_1 - b_1 + a_1 b_1^2. \end{array} \tag{3.7}$$

which is precisely the original system (1.2) with

$$a = a_1, \qquad b = b_1, \qquad \varepsilon = r_1.$$

Thus, the geometric singular perturbation analysis of Regime 1 is valid on compact regions in chart K_1.

Remark 3.2. *Writing system (3.1) in chart K_1 corresponds to undoing the scaling (2.3). This explains also the choice of the weights, i.e. the r-factors, in the blow-up transformation (3.2). The blow-up transformation has to be chosen such that the rescaling (2.3) corresponds to the blow-up transformation (3.3) in chart K_1 defined by $\bar{\varepsilon} = 1$.*

Dynamics in chart K_2. Applying transformation (3.4) to system (3.1) and desingularizing by dividing out the factor r_2, we obtain

$$\begin{array}{lcl} a_2' & = & -r_2(a_2 + \varepsilon_2^2 a_2 - \varepsilon_2^2 \mu), \\ r_2' & = & r_2(a_2 + \varepsilon_2^2 a_2 - \varepsilon_2), \\ \varepsilon_2' & = & -\varepsilon_2(a_2 + \varepsilon_2^2 a_2 - \varepsilon_2), \end{array} \tag{3.8}$$

where $'$ denotes differentiation with respect to a rescaled time variable t_2. System (3.8) has two invariant subspaces, namely the plane $\varepsilon_2 = 0$ and the plane $r_2 = 0$.

The dynamics in the invariant plane $\varepsilon_2 = 0$ is governed by

$$\begin{array}{lcl} a_2' & = & -a_2 r_2, \\ r_2' & = & a_2 r_2. \end{array} \tag{3.9}$$

The r_2-axis and the a_2-axis are two lines of equilibria, which we denote by L_B and L_A, respectively. The line L_B corresponds to the normally hyperbolic line l_B. Away from $(a_2, r_2) = (0, 0)$ the line L_B is attracting for the flow in $\varepsilon_2 = 0$. The new line of equilibria L_A is repelling for the flow in $\varepsilon_2 = 0$. Thus, the dynamics in $\varepsilon_2 = 0$ is very similar to the dynamics of the layer problem (2.5), but with the normally hyperbolic line L_A instead of the non-hyperbolic line l_A, see Figure 7.

In the invariant plane $r_2 = 0$ system (3.8) reduces to

$$\begin{array}{lcl} a_2' & = & 0, \\ \varepsilon_2' & = & -(a_2 + \varepsilon_2^2 a_2 - \varepsilon_2)\varepsilon_2. \end{array} \tag{3.10}$$

The equilibria of this system are the line L_A and a curve of equilibria corresponding to the critical manifold S from Section 2. Recall that S consists of an attracting branch S_a and a repelling branch S_r separated by the non-hyperbolic fold point p_f. Within $r_2 = 0$ the line L_A is attracting i.e. there exist heteroclinic orbits from S_r to L_A in $r_2 = 0$.

Remark 3.3. *Note that the repelling slow manifold S_r and the unstable fiber of the fold point p_f, which are unbounded in Regime 1, have been compactified in chart K_2.*

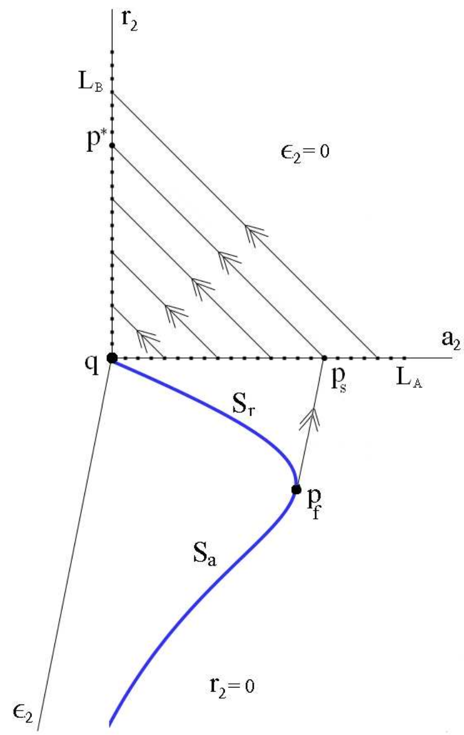

FIGURE 7. Dynamics of system (3.8) in $\varepsilon_2 = 0$ and $r_2 = 0$.

Lemma 3.1. *The following assertions hold for system (3.8):*

(1) *The linearization at the steady states in L_B has a double zero eigenvalue and a simple eigenvalue $-r_1$ with eigenspaces span$\{(0,1,0)^T,(0,0,1)^T\}$ and span$\{(-1,1,0)\}$.*
(2) *The line L_A is a line of hyperbolic steady states of saddle type.*
(3) *The linearization of the system (3.8) at the origin has a triple zero eigenvalue.*

Proof. Computations. □

Property 1 of the lemma suggests the existence of an attracting two-dimensional invariant manifold containing the line L_B as long as r_2 is bounded away from zero. Since the region $r_2 \geq \delta$ corresponds to $B \geq \delta$ this manifold is precisely the slow manifold described in Theorem 2.2. Thus, we conclude

Lemma 3.2. *Let $\delta > 0$. For $r_2 \geq \delta$ system (3.8) has an exponentially attracting two-dimensional slow manifold M containing the line of equilibria L_B. The manifold M is given as a graph $a_2 = \mu\varepsilon_2^2 + O(r_2^3\varepsilon_2^3)$. There exists a stable foliation $\mathcal{F}$ with base M and one-dimensional fibers. The contraction along $\mathcal{F}$ in a time interval of length t is stronger than e^{-ct} for any $0 < c < \delta$. For the slow flow on M the variable r_2 is strictly decreasing.*

Note that away from the origin the line L_A has gained hyperbolicity due to the blow up in contrast to the situation for the line l_a for system (2.5). The origin is still a very degenerate equilibrium of system (3.2) which will be studied later by means of further blow-up (Appendix A).

3.2. **Dynamics of the blown-up system.** The above analysis provides us with the following picture of the dynamics of the blown-up vector field shown in Figure 8. We find the critical manifold S with its attracting and repelling branches S_a, S_r on the cylinder and the lines L_B, L_A of equilibria.

There are five particular points, denoted by $p_* \in S_a$, $p_f \in S$, $p_s \in L_A$, $p^* \in L_B$, $q \in L_A \cap L_B \cap S_r$. The point p_f is the fold point of S and the other points are described below. We introduce the following notation: ω_1 is the segment of S_a from p_* to p_f; ω_2 is the heteroclinic orbit of system (3.9) connecting p_f to p_s; ω_3 is the union of p_s and the heteroclinic orbit of system (3.10) connecting p_s to p^*; ω_4 is the segment of L_B connecting p^* to q; ω_5 is the heteroclinic orbit connecting q with p_* on the cylinder $r = 0$, which is described by system (3.9) close to q and by (3.7) close to p_*.

We define the singular cycle $\Gamma_0 = \omega_1 \cup \omega_2 \cup \omega_3 \cup \omega_4 \cup \omega_5$. Note that due to the blow-up the singular cycle γ_0 of Theorem 2.3 has been replaced by the more complicated singular cycle Γ_0. Due to the improved hyperbolicity properties of Γ_0 we can show that Γ_0 persists as a genuine periodic orbit for ε small. Since $\varepsilon = r\bar{\varepsilon}$ we have to analyze the blown-up vector field for r small or $\bar{\varepsilon}$ small, i.e. close to the cylinder $r = 0$ or close to the invariant plane $\bar{\varepsilon} = 0$, respectively.

Theorem 3.1. *For $\mu > 1$ the blown-up vector field $\bar{X}$ has a family of attracting periodic orbits $\bar{\Gamma}_\varepsilon$ parameterized by $\varepsilon \in (0, \varepsilon_0]$, ε_0 sufficiently small, which for $\varepsilon \to 0$ tend to the singular cycle $\Gamma_0 = \omega_1 \cup \omega_2 \cup \omega_3 \cup \omega_4 \cup \omega_5$.*

Remark 3.4. *Theorem 2.3 follows from Theorem 3.1 by applying the blow-up transformation (3.2).*

4. Construction of the Poincaré map

In this section we prove Theorem 3.1 by showing that an appropriately defined Poincaré map possesses an attracting fixed point. The Poincaré map will be constructed as the composition of five local transition maps defined in suitable neighborhoods of the singular cycle Γ_0. The five local transition maps are discussed in detail in Subsections 4.1 – 4.5.

We choose sections Σ_i, $i = 1, \ldots, 5$ as shown in Figure 8, i.e.
Σ_1 is transversal to the curve of steady states S_a and close to the fold point p_f;
Σ_2 is transversal to the heteroclinic orbit ω_2 and close to p_s;
Σ_3 is transversal to the heteroclinic orbit ω_3 and close to the line L_B;
Σ_4 is transversal to the line L_B and close to the nilpotent point q;
Σ_5 is transversal to the heteroclinic orbit ω_5 and close to q.

The sections Σ_i will be defined more precisely in Subsections 4.1 – 4.5, where the blown up system is considered in specific charts.

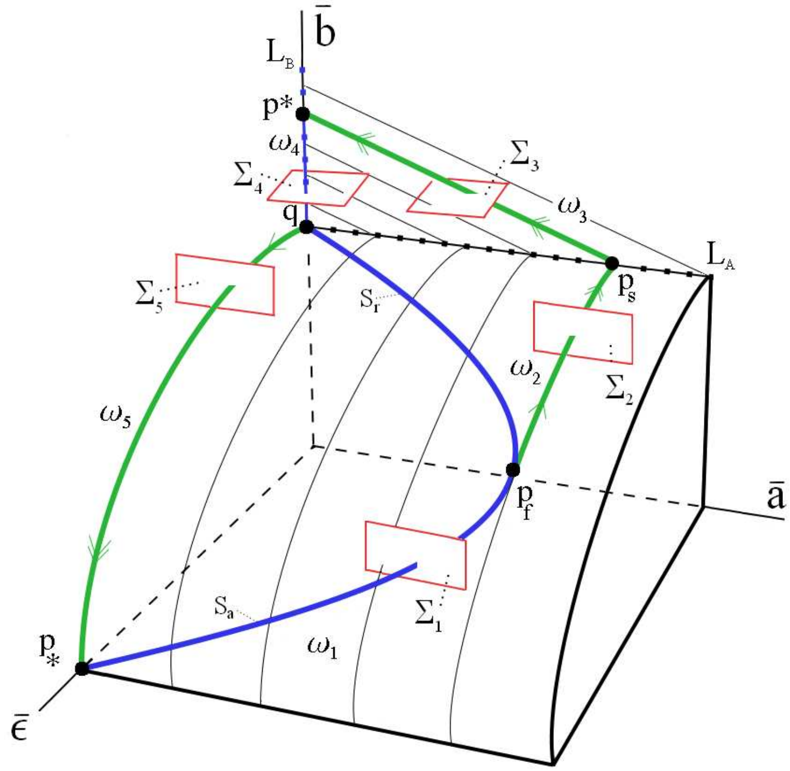

FIGURE 8. Dynamics of the blown-up system, singular cycle Γ_0, and sections.

We introduce the following maps defined by the flow of $\bar{X}$:

$\Pi_1 : \Sigma_1 \to \Sigma_2$ – passage of the fold point p_f,
$\Pi_2 : \Sigma_2 \to \Sigma_3$ – passage of the hyperbolic line L_A,
$\Pi_3 : \Sigma_3 \to \Sigma_4$ – contraction onto the vertical slow manifold,
$\Pi_4 : \Sigma_4 \to \Sigma_5$ – passage of the nilpotent point q,
$\Pi_5 : \Sigma_5 \to \Sigma_1$ – contraction onto the attracting slow manifold.

We will show that the map $\Pi : \Sigma_1 \to \Sigma_1$ defined as

$$\Pi = \Pi_5 \circ \Pi_4 \circ \Pi_3 \circ \Pi_2 \circ \Pi_1$$

is a contraction with a fixed point.

Let $\delta > 0$, $\beta_1 > 0$, $\beta_2 > 0$ and α_i be fixed small numbers, which will be used in the definition of all sections Σ_i, $i = 1, \dots, 5$.

4.1. **Analysis of Π_1 – passage of the fold point.** The construction of the transition map Π_1 is carried out in chart K_1, i.e. the dynamics is governed by system (3.7), which is the original system (1.2) with $a = a_1,\ b = b_1,\ \varepsilon = r_1$. We define

$$\Sigma_1 = \left\{(a_1, b_1, r_1) : a_1 = \tfrac{1}{2} - \delta,\ b_1 \in [0, \tfrac{1}{2}],\ r_1 \in [0, \beta_1]\right\}$$

and

$$\Sigma_2 = \{(a_1, b_1, r_1) : |\tfrac{1}{2} - a_1| \le \alpha_2,\ b_1 = 1/\delta,\ r_1 \in [0, \beta_1]\}.$$

For ε sufficiently small all orbits starting in Σ_1 are rapidly attracted by the slow manifold $S_{a,\varepsilon}$ from Theorem 2.1. The analysis in [13] implies that the continuation of $S_{a,\varepsilon}$ intersects Σ_2 transversally. Hence, the map Π_1 is well defined. By combining the analysis of the generic fold point in [13] with standard Fenichel theory [7] we obtain

Theorem 4.1. *For fixed $\delta > 0$ there exists $\beta_1 > 0$ such that the transition map*

$$\Pi_1 : \Sigma_1 \to \Sigma_2 \tag{4.1}$$

is defined. The transition map Π_1 is exponentially contracting, i.e. for r_1 fixed the a_1 component of the map is contracting with rate e^{-c_1/r_1} with a constant $c_1 > 0$.

4.2. **Analysis of Π_2 – passage of the hyperbolic line L_A.** We now analyze the dynamics close to the point $p_s \in L_A$. The construction of the transition map Π_2 is carried out in chart K_2, i.e. the dynamics is governed by system (3.8).

In K_2 the section Σ_2 is a subset of the plane $\varepsilon_2 = \delta$. We define the section Σ_3 by

$$\Sigma_3 = \{(a_2, r_2, \varepsilon_2) : |\tfrac{1}{2} - a_2| \le \alpha_3,\ r_2 = \delta,\ \varepsilon_2 \in [0, \beta_2]\}.$$

Let $p_0 = (\frac{1}{2}, 0, \delta) \in \Sigma_2$ denote the point where the singular cycle Γ_0 intersects the section Σ_2. Let $R_2 \in \Sigma_2$ be an arbitrarily small rectangle centered at p_0, see Figure 9. Recall that the invariant plane $r_2 = 0$ corresponds to the cylinder and that the plane $\varepsilon_2 = 0$ is invariant.

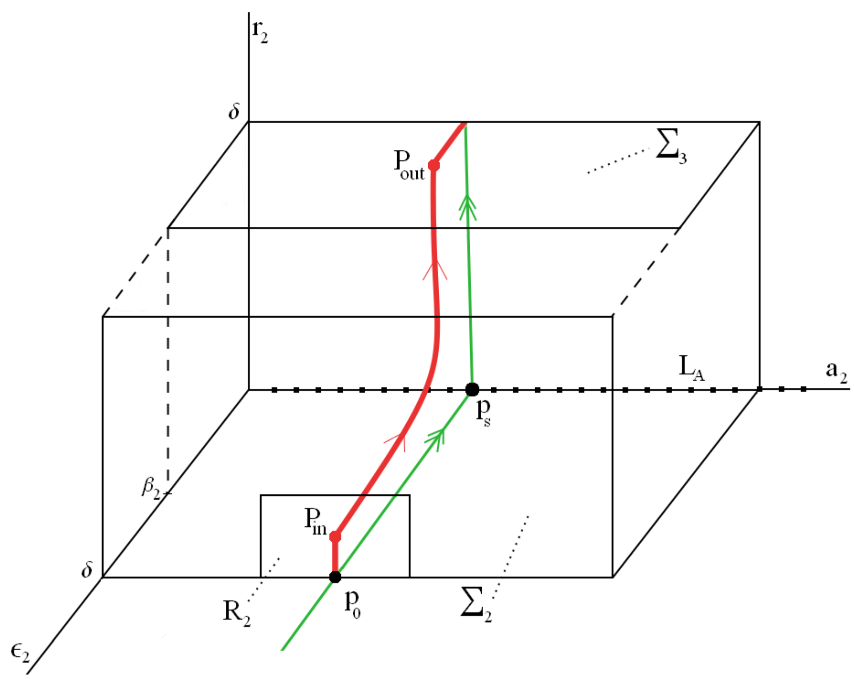

FIGURE 9. Passage of the hyperbolic line L_A.

For computational purposes we shift the point p_s to the origin by making the change of coordinates $\tilde{a}_2 = a_2 - \frac{1}{2}$. For the sake of readability we omit the subscript of the variables in this subsection. In these variables the system has the form

$$\begin{aligned} \tilde{a}' &= -r - 2r\varepsilon G(\varepsilon, \tilde{a}), \\ r' &= r, \\ \varepsilon' &= -\varepsilon \end{aligned} \tag{4.2}$$

with

$$G(\tilde{a}, \varepsilon) := \frac{(1 - \mu\varepsilon)}{1 + 2\tilde{a} + 2\varepsilon^2(\tilde{a} + 1/2) - 2\varepsilon},$$

where we have divided the vector field by the factor $F(\tilde{a}, r, \varepsilon) = \tilde{a} + \frac{1}{2} + \varepsilon^2(\tilde{a} + \frac{1}{2}) - \varepsilon$ which does not vanish in a small neighborhood of the origin. For this system the origin is a non-hyperbolic equilibrium whose eigenvalues are $-1, 1, 0$ and are in resonance $(-1+1=0)$. This indicates that the resonant terms in (4.2) cannot be eliminated by a normal form transformation and that the transition map is difficult to compute due to the occurrence of logarithmic terms. However, we are able to show

Theorem 4.2. *For system (3.8) the transition map*

$$\Pi_2 : R_2 \to \Sigma_3, \qquad (a_{in}, r_{in}, \delta) \mapsto (a_{out}, \delta, r_{in})$$

is well defined for δ small enough and sufficiently small rectangle $R_2 \subset \Sigma_2$, and satisfies

$$a_{in} + r_{in} - \delta - 2(1+c_2)\delta r_{in} \ln r_{in} \;\le\; a_{out} \;\le\; a_{in} + r_{in} - \delta, \tag{4.3}$$

where the constant $c_2 > 0$ can be made arbitrarily small for δ small. The map Π_2 restricted to the line $r_{in} = const.$ is at most algebraically expanding.

Proof. In the proof we use the system (4.2) with the shifted variable $\tilde{a} = a - \frac{1}{2}$. To estimate a_{out} for given $(r_{in}, a_{in}) \in \Sigma_2$ consider a solution $(\tilde{a}, r, \varepsilon)(t)$ of (4.2) which satisfies

$$\begin{array}{rclcrcl} \tilde{a}(0) & = & \tilde{a}_{in}, & & \tilde{a}(T) & = & \tilde{a}_{out}, \\ r(0) & = & r_{in}, & & r(T) & = & \delta, \\ \varepsilon(0) & = & \delta, & & \varepsilon(T) & = & \varepsilon_{out}. \end{array} \tag{4.4}$$

The formulas $\varepsilon(t) = \delta e^{-t}$ and $r(t) = r_{in} e^t$ imply that the transition time T is given by

$$T = \ln \frac{\delta}{r_{in}}. \tag{4.5}$$

Since $0 \le G(\tilde{a}, \varepsilon) \le 1 + c_2$ with $c_2 > 0$ small for δ small, we obtain the inequality

$$-r_{in} e^t - 2\delta r_{in}(1+c_2) \le a' \le -r_{in} e^t$$

by using the formulas for $r(t)$ and $\varepsilon(t)$. Inequality 4.3 follows by integrating and using the initial conditions and the formula for the transition time.

Since $\tilde{a}$ satisfies the scalar non-autonomous differential equation

$$\tilde{a}' = r_{in} e^t - 2\delta r_{in} G(\delta e^{-t}, \tilde{a}),$$

$\tilde{a}_{out}$ depends Lipschitz continuously on $\tilde{a}_{in}$ on a line $r_{in} = const.$ with a Lipschitz constant of the order r_{in}^{-L} for some constant L.

□

4.3. **Analysis of Π_3 – contraction towards the vertical slow manifold M.** The construction of the transition map Π_3 is carried out in chart K_2, i.e. the dynamics is governed by system (3.8) in the variables $(a_2, r_2, \varepsilon_2)$. We define Σ_4 by

$$\Sigma_4 = \{(a_2, r_2, \varepsilon_2) : |a_2| \le \alpha_4,\ r_2 = \delta,\ \varepsilon_2 \in [0, \beta_2]\}$$

with β_2 and $\alpha_4 > 0$ small. For $B = r_2 \ge \delta$ the system is equivalent to system (2.4) and Lemma 3.2 is applicable for $\varepsilon = r_2\varepsilon_2$ small enough, which can be guaranteed by choosing β_2 small.

We conclude that all orbits starting in Σ_3 are rapidly attracted by the slow manifold M, follow the slow flow downwards, and intersect Σ_4. More precisely we have

Theorem 4.3. *For $\delta > 0$ there exists β_2 small enough such that*

(1) *The transition map*

$$\Pi_3 : \Sigma_3 \to \Sigma_4, \qquad (a_{2,in}, \delta, \varepsilon_{2,in}) \mapsto (a_{2,out}, \delta, \varepsilon_{2,in})$$

is well defined. Restricted to lines $\varepsilon_{2,in} = const.$ *in* Σ_3 *the map* Π_3 *is contracting with a rate* e^{-c_3/ε_2} *with* $c_3 > 0$ *as* $\varepsilon_{2,in} \to 0$.

(2) *The intersection of* M *with* Σ_4 *is a smooth curve* σ_4 *given by* $a_2 = \mu\varepsilon_2^2 + O(\varepsilon_2^3\delta^3)$.

(3) *The image* $\Pi_3(\Sigma_3)$ *is an exponentially thin wedge lying exponentially close to the curve* σ_4.

Proof. Since $r_{2,in} = r_{2,out} = \delta$ the relation $\varepsilon = r_2\varepsilon_2$ implies $\varepsilon_{2,out} = \varepsilon_{2,in}$. The other assertions of the theorem follow from standard Fenichel theory. □

4.4. **Analysis of Π_4 – passage of the nilpotent point q.** The construction of the transition map Π_4 is carried out in chart K_2. We define the section Σ_5

$$\Sigma_5 = \{(a_2, r_2, \varepsilon_2) : |a_2| \le \alpha_5,\ r_2 \in [0, \beta_1/\delta],\ \varepsilon_2 = \delta\}.$$

Let $R_4 \subset \Sigma_4$ be an arbitrarily small rectangle centered at the origin where the singular cycle Γ_0 intersects Σ_4.

Theorem 4.4. *For* δ *small enough and a sufficiently small rectangle* $R_4 \subset \Sigma_4$ *the transition map* $\Pi_4 : R_4 \to \Sigma_5$ *is a* C^1*- map and has the following properties*

(1) *The continuation of* M *by the flow intersects* Σ_5 *in a* C^1*-curve* σ_5 *which is tangent to* $r_2 = 0$.

(2) *Restricted to lines* $\varepsilon_2 = const.$ *in* R_4 *the map* Π_4 *is contracting with a rate* e^{-c_4/ε_2} *with* $c_4 > 0$ *as* $\varepsilon_{2,in} \to 0$.

(3) *The image* $\Pi_4(R_4)$ *is an exponentially thin wedge containing the curve* σ_5.

Proof. The proof based on blowing up the point q is given in Appendix A. □

4.5. **Analysis of Π_5 – transition towards the attracting slow manifold S_a.** We now analyze the transition map from Σ_5 to Σ_1. This is done in chart K_1, where the dynamics is described by system (3.7). Recall that system (3.7) is just the original system (1.2) where $\varepsilon = r_1$ is constant along the flow. In K_1 the section Σ_5 is given by

$$\Sigma_5 = \{(a_1, b_1, r_1) : |a_1| \le \alpha_5,\ b_1 = 1/\delta,\ r_1 \in [0, \beta_1]\}.$$

For β_1 small the analysis from Regime 1 implies that all orbits starting from $(a_{in}, \frac{1}{\delta}, \varepsilon) \in \Sigma_5$ are attracted by the slow manifold $S_{a,\varepsilon}$, follow the slow dynamics along $S_{a,\varepsilon}$ and after a while cross the section Σ_1 transversally. More precisely we have

Theorem 4.5. *For* $\delta > 0$ *there exists* β_1 *small such that*

(1) *The transition map* $\Pi_5 : \Sigma_5 \to \Sigma_1$ *is well defined.*

(2) *Its restriction to a slice* $\varepsilon = const.$ *is a contraction with the contraction rate* $O(e^{-c_5/\varepsilon})$, *where* $c_5 > 0$.

(3) *The image* $\Pi_5(\Sigma_5)$ *is an exponentially thin wedge lying exponentially close to the smooth curve formed by the intersection of the family* $S_{a,\varepsilon}$ *with* Σ_1.

4.6. **Proof of Theorem 3.1.**

Proof. It follows from Theorems 4.1-4.5 that for β_1 sufficiently small the transition map $\Pi : \Sigma_1 \to \Sigma_1$ given by

$$\Pi = \Pi_5 \circ \kappa_{21} \circ \Pi_4 \circ \Pi_3 \circ \Pi_2 \circ \kappa_{12} \circ \Pi_1$$

is well defined. In this formula the coordinate changes are needed because Π_1 and Π_5 have been defined in chart K_1, while Π_2, Π_3 and Π_4 have been defined in chart K_2.

Since ε is a constant of motion for the blown-up system lines $\varepsilon = const.$ are invariant under the map Π. Since the maps Π_1, Π_3, Π_4, Π_5 are exponentially contracting on lines $\varepsilon = const.$ and Π_2 is at most algebraically expanding, the map Π restricted to $\varepsilon = const.$ is exponentially contracting. The contraction mapping theorem implies the existence of a unique fixed point corresponding to an exponentially attracting periodic orbit $\bar{\Gamma}_\varepsilon$ of the blown-up vector field close to the singular cycle Γ_0 for ε sufficiently small. □

5. Canard cycles

As the parameter μ passes through $\mu = 1$ the a-nullcline of system 1.1 crosses the fold point p_f of the critical manifold S. According to [13] the non-hyperbolic point p_f is a *canard point* for $\mu = 1$. The corresponding reduced flow on the critical manifold S is smooth at the point p_f and passes through the fold point, see Fig. 2. It has been shown in [1], [4], and [13] that this configuration implies the existence of canard solutions and the occurence of a canard explosion for $\mu \approx 1$ and ε small. Canard solutions correspond to situations where the slow manifolds $S_{a,\varepsilon}$ and $S_{r,\varepsilon}$ are exponentially close in a neighborhood of p_f. A canard colution is a solution which is initially attracted by $S_{a,\varepsilon}$, passes the fold point and follows the repelling slow manifold $S_{r,\varepsilon}$ for a while before it is finally repelled from $S_{r,\varepsilon}$. A canard solution which forms a closed cycle is called a canard cycle. Canard explosion is the phenomenon that a small limit cycle is generated in a Hopf-bifurcation at $\mu = \mu_{Hopf}(\varepsilon)$ and grows to a large relaxation cycle as μ varies in an exponentially small interval.

As μ grows the following types of canard cycles of System 1.1 exist, see Fig. 8:

(1) Canard cycles corresponding to singular cycles which start at a point on S_a, pass through p_f, follow S_r and jump back to the starting point on S_a.
(2) Canard cycles corresponding to the singular cycle which start at $p_* \in S_a$, pass through p_f, follow S_r until the point q and jump back to $p_* \in S_a$.
(3) Canard cycles corresponding to singular cycles which start on S_a, pass through p_f, follow S_r, jump to the line L_A, jump to the line L_B, follow the slow flow on L_B downwards to the point q and jump back to the point $p_* \in S_a$. This type of canards limits on the relaxation cycles corresponding to $\mu > 1$ considered in this paper.

Canard cycles of Type 1 are covered by the results in [13].

Canard cycles of Type 3 can be analyzed by combining results on canard points from [13] with the return mechanism discussed in this paper corresponding to the map $\Sigma_2 \to \Sigma_5$ (with an in a-direction suitably extended section Σ_2).

The analysis of intermediate canard cycles of Type 2 is more subtle and requires a more detailed analysis of the system from Appendix A obtained by blowing up the nilpotent point q, see Figure 11.

Acknowledgement

The authors would like to thank Alexandra Milik for helpful discussions on this problem during the early stage of this research.

References

[1] E. F. Benoit, J. F. Callot, F. Diener and M. Diener, *Chasse au canard*, Collectanea Mathematica, **31-32** (1981), 37–119.

[2] M. Brons, M. Krupa and M. Wechselberger, *Mixed mode oscillations due to the generalized canard phenomenon*, Bifurcation theory and spatio-temporal pattern formation, Fields Inst. Commun., Amer. Math. Soc., Providence, RI, **49** (2006), 39–63.

[3] S.-N. Chow, C. Li and D. Wang, "Normal Forms and Bifurcation of Planar Vector Fields", Cambridge University Press, Cambridge, 1994.

[4] F. Dumortier and R. Roussarie, *Canard cycles and center manifolds*, Mem. Amer. Math. Soc., Providence, **577** (1996).

[5] F. Dumortier and R. Roussarie, *Multiple canard cycles in generalized Liénard equations*, J. Differential Equations, **174** (2001), 1–29.

[6] F. Dumortier, N. Popovic and T. J. Kaper, *The critical wave speed for the Fisher-Kolmogorov-Petrowskii-Piscounov equation with cut-off*, Nonlinearity, **20** (2007), 855–877.

[7] N. Fenichel, *Geometric singular perturbation theory*, J. Differential Equations, **31** (1979), 53–98.

[8] J. Grasman, "Asymptotic Methods for Relaxation Oscillations and Applications", Springer, New York, 1987.

[9] J. Guckenheimer and P. Holmes, "Nonlinear Oscillations, Dynamical Systems, and Bifurcations of Vector Fields", Springer, New York, 1983.

[10] A. Huber and P. Szmolyan, *Geometric singular perturbation analysis of the Yamada model*, SIAM J. Appl. Dyn. Syst., **4** (2005), 607–648.

[11] C.K.R.T. Jones, *Geometric singular perturbation theory*, Springer Lecture Notes in Mathematics, Berlin, **(1609)** 1995, 44–120.

[12] M. Krupa, N. Popovic, N. Kopell and H.G. Rotstein, *Mixed-mode oscillations in a three time-scale model for the dopaminergic neuron*, Chaos, **18** (2008), 015106–015106-19.

[13] M. Krupa and P. Szmolyan, *Extending geometric singular perturbation theory to non-hyperbolic points-fold and canard points in two dimensions*, SIAM J. Math. Analysis, **33** (2001), 286–314.

[14] M. Krupa and P. Szmolyan, *Relaxation oscillation and canard explosion*, J. Differential Equations, **174** (2001), 312–368.

[15] P. De Maesschalck and F. Dumortier, *Canard solutions at non-generic turning points*, Trans. Amer. Math. Soc., **358** (2006), 2291–2334.

[16] A. Milik, "Mixed-Mode Oscillations in Chemical Systems", Ph.D thesis, Vienna University of Technology, 1996.

[17] A. Milik and P. Szmolyan, *Multiple time scales and canards in a chemical oscillator*, Multiple-time-scale dynamical systems, IMA Vol. Math. Appl., Springer, New York, **122** (2001), 117–140.

[18] A. Milik, P. Szmolyan, H. Löffelmann and E. Gröller, *Mixed mode oscillations in chemical systems*, Internat. J.Bifurcations and Chaos, **8** (1998), 505–519.

[19] E.F. Mishchenko and N.Kh. Rozov, "Differential Equations with Small Parameters and Relaxation Oscillations", Plenum Press, New York, 1980.

[20] V. Petrov, S.K. Scott and K. Showalter, *Mixed-mode oscillations in chemical systems*, Journal of Chemical Physics, **97** (1992), 6191–6198.

[21] N. Popovic and P. Szmolyan, *A geometric analysis of the Lagerstrom model problem*, J. Differential Equations, **199** (2004), 290–325.

[22] S.K. Scott, *Chemical Chaos*, International series of monographs on chemistry, Oxford University Press, **24** (1991).

[23] S. Sternberg, *On the structure of local homeomorphisms of euclidean n-space II*, Amer. J. Math., **80** (1958), 623–631.

[24] P. Szmolyan and M. Wechselberger, *Canards in $\mathbb{R}^3$*, J. Differential Equations, **177** (2001), 419–453.

Appendix A. Passage of the nilpotent point q

Here we construct the transition map $\Pi_4 : R_4 \to \Sigma_5$ and prove Theorem 4.4. Since the construction of the transition map Π_4 is done in chart K_2 only, we omit the subscript $_2$ of the variables for the sake of readability. Hence, the governing equations are

$$\begin{array}{rcl} a' &=& -r(a+\varepsilon^2 a_2 - \varepsilon^2\mu), \\ r' &=& r(a+\varepsilon^2 a_2 - \varepsilon), \\ \varepsilon' &=& -\varepsilon(a+\varepsilon^2 a - \varepsilon). \end{array} \tag{A.1}$$

We know from Section 3 (Lemma 3.1) that $q = (0,0,0)$ is an equilibrium of system (A.1) with a triple zero eigenvalue. To analyze this degenerate equilibrium we again use the blow-up method. We use the radial homogeneous blow-up

$$\begin{array}{rcl} a &=& \rho\bar{a}, \\ r &=& \rho\bar{r}, \\ \varepsilon &=& \rho\bar{\varepsilon}, \end{array} \tag{A.2}$$

where $(\bar{a},\bar{r},\bar{\varepsilon}) \in \mathbb{S}^2$ and $\rho \in [0,\rho_0]$ for ρ_0 sufficiently small, i.e. the origin is blown-up to a two-sphere, see Figure 10. The analysis of the blown-up vector field is

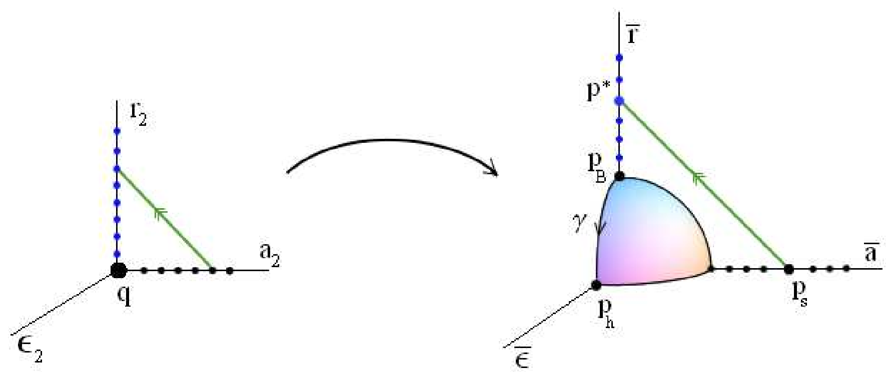

Figure 10. Blow-up transformation (A.2) for system (A.1).

again carried out in two charts $\mathcal{K}_1$ and $\mathcal{K}_2$ defined by setting $\bar{r} = 1$ and $\bar{\varepsilon} = 1$, respectively. The blow-up transformation is given by

$$a = \rho_1 a_1, \qquad r = \rho_1, \qquad \varepsilon = \rho_1\varepsilon_1, \tag{A.3}$$

in chart $\mathcal{K}_1$ and by

$$a = \rho_2 a_2, \qquad r = \rho_2 r_2, \qquad \varepsilon = \rho_2 \tag{A.4}$$

in chart $\mathcal{K}_2$. The change of coordinates from $\mathcal{K}_1$ to $\mathcal{K}_2$ is given by

$$\begin{array}{rcl} \rho_2 &=& \varepsilon_1\rho_1, \\ a_2 &=& a_1\varepsilon_1^{-1}, \\ r_2 &=& \varepsilon_1^{-1}. \end{array} \tag{A.5}$$

The section Σ_4 from Subsection 4.4 written in chart $\mathcal{K}_1$ lies in the plane $\rho_1 = \delta$, similarly the section Σ_5 written in chart $\mathcal{K}_2$ lies in the plane $\rho_2 = \delta$.

The dynamics in chart $\mathcal{K}_1$ is governed by

$$\begin{array}{rcl} a_1' &=& -a_1 - a_1^2 + \varepsilon_1 a_1 + \rho_1\varepsilon_1^2\mu - \varepsilon_1^2 a_1\rho_1^2(a_1+1), \\ \rho_1' &=& a_1\rho_1 + \varepsilon_1^2 a_1\rho_1^3 - \varepsilon_1\rho_1, \\ \varepsilon_1' &=& 2\varepsilon_1(\varepsilon_1 - a_1) - 2\rho_1^2 a_1\varepsilon_1^3. \end{array} \tag{A.6}$$

We recover the line of steady states $L_B = \{(0, \rho_1, 0),\ \rho_1 \geq 0\}$ of system (A.1). We denote the steady state at $(0,0,0) \in L_B$ by p_B. Furthermore, the planes $\varepsilon_1 = 0$, $\rho_1 = 0$ and the ε_1- and a_1-axes are invariant under the flow (A.6).

In chart $\mathcal{K}_1$ the rectangle R_4 is defined by

$$R_4 = \{(a_1, \rho_1, \varepsilon_1) : a_1 \in [0, \tilde{\alpha}],\ \rho_1 = \delta,\ \varepsilon_1 \in [0, \tilde{\alpha}]\}.$$

Lemma A.1. *The following assertions hold for system (A.6):*

(1) *The linearization of system (A.6) at the steady states in L_B has a stable eigenvalue -1 and a double zero eigenvalue. The associated stable and center eigenspaces are $E_b^s = (1,0,0)^T$ and $E_b^c = span\{(0,0,1)^T, (0,1,0)^T\}$.*

(2) *There exists a two-dimensional center manifold $\mathcal{M}$ at p_B which contains the line of steady states L_B and the invariant ε_1-axis. In $\mathcal{K}_1$ the manifold is given as a graph $a_1 = h(\rho_1, \varepsilon_1) = \mu\rho_1\varepsilon_1^2 + O(\varepsilon_1^3\rho_1^5)$. The center manifold $\mathcal{M}$ can be chosen to be the continuation of M from Lemma 3.2 by the flow.*

(3) *The manifold $\mathcal{M}$ is an attracting center manifold. All orbits starting from R_4 are exponentially attracted onto $\mathcal{M}$.*

Proof. Assertion (1) follows from simple computations. Assertion (2) – (4) follows from center manifold theory [3], [9] applied at the point p_B which has gained an attracting direction due to the blow-up. □

The dynamics in $\mathcal{K}_2$ is governed by

$$\begin{aligned} a_2' &= a_2^2 - a_2 - a_2 r_2 + r_2\mu\rho_2 + a_2\rho_2^2(a_2 - r_2), \\ r_2' &= -2r_2 + 2a_2 r_2 + 2a_2 r_2 \rho_2^2, \\ \rho_2' &= \rho_2(1 - a_2) - \rho_2^3 a_2. \end{aligned} \tag{A.7}$$

The system has an equilibrium at the origin, which we denote by p_h. The planes $r_2 = 0$, $\rho_2 = 0$ and the a_2-, r_2- and ρ_2-axes are invariant under the flow.

Lemma A.2. *The linearization at the equilibrium p_h is hyperbolic with the eigenvalues -1, -2 and 1 with eigenvectors $(1,0,0)^T$, $(0,1,0)^T$ and $(0,0,1)^T$, respectively.*

This implies that there exists a heteroclinic orbit γ of the blown-up vector field on the sphere connecting p_B to p_h, which corresponds to the ε_1-axis in $\mathcal{K}_1$ and to the r_2-axis in $\mathcal{K}_2$, see Figures 10 and 11. To prove Theorem 4.4 we have to study how orbits starting in R_4 pass the non-hyperbolic point p_B, follow the heteroclinic orbit across the sphere and exit close to the hyperbolic point p_h where they intersect Σ_5 by following the unstable $\bar{\varepsilon}$-direction. It turns out that the behavior of all orbits is determined by the behavior of the continuation of the center manifold $\mathcal{M}$ which attracts all other orbits.

To study the dynamics near p_B, we define the section Σ_{loc} in chart $\mathcal{K}_1$ by

$$\Sigma_{loc} = \big\{(a_1, \rho_1, \varepsilon_1) : a_1 \in [0, \alpha],\ \rho_1 \in [0, \delta],\ \varepsilon_1 = \alpha\big\}.$$

To study the dynamics near p_h, we define the section Σ_{in} in $\mathcal{K}_2$ by

$$\Sigma_{in} = \{(a_2, r_2, \rho_2) : a_2 \in [0, \alpha],\ r_2 = \alpha,\ \rho_2 \in [0, \delta]\}.$$

In $\mathcal{K}_1$ the section Σ_{in} lies in the plane $\varepsilon_1 = 1/\alpha$.

The transition map Π_4 will be obtained as the composition of a local transition map π_1 from R_4 to Σ_{loc}, a global transition map π_2 from Σ_{loc} to Σ_{in} and a local transition map π_3 from Σ_{in} to Σ_5, see Figure 11.

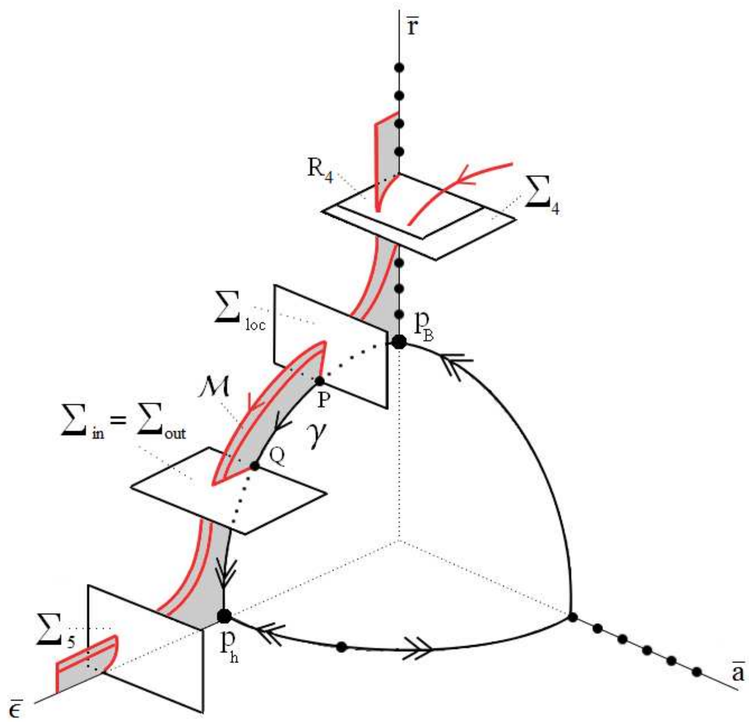

FIGURE 11. Blown-up phase space $\mathbb{S}^2 \times [0, \rho_0]$ for system (A.1): sections, slow manifold $\mathcal{M}$ and an orbit which is attracted to $\mathcal{M}$.

Analysis of π_1. Here we work in chart $\mathcal{K}_1$. At the point p_B the dynamics of system (A.6) is controlled by the attracting center manifold $\mathcal{M}$ from Lemma A.1 and we conclude the following.

Lemma A.3. *For δ and α sufficiently small the transition map $\pi_1 : R_4 \to \Sigma_{loc}$ is a smooth map with the properties:*

(1) *The intersection of $\mathcal{M}$ with Σ_{loc} is a smooth curve given by $a_1 = \mu\rho_1\alpha^2 + O(\alpha^3\rho_1^5)$.*
(2) *Restricted to lines $\varepsilon_1 = const.$ the map π_1 is exponentially contracting with a rate e^{-c/ε_1} with a constant $c > 0$.*

Analysis of π_2. We are still working in chart $\mathcal{K}_1$. In the blown-up system the singular orbit Γ_0 intersects the section Σ_{loc} in the point $P = (0, 0, \alpha)$ and Σ_{in} in the point $Q = (0, 0, \frac{1}{\alpha})$, hence orbits staring in Σ_{loc} intersect Σ_{in}. More precisely, we have

Lemma A.4. *For δ and α sufficiently small the map $\pi_2 : \Sigma_{loc} \to \Sigma_{in}$ is a diffeomorphism. The intersection of the continuation of $\mathcal{M}$ with Σ_{in} is a smooth curve with tangent vector $t_Q = (\sqrt{1/\alpha}, \sqrt{\alpha}, 0)^T$ at the point Q.*

Proof. For δ and α sufficiently small all orbits starting in Σ_{loc} reach Σ_{in} in finite time hence π_2 is a diffeomorphism.

To have some information on the continuation of $\mathcal{M}$, we compute the evolution of its tangent space along the heteroclinic orbit γ. We parametrize γ by

$$\gamma = \{(0, 0, \varepsilon_1),\ \varepsilon_1 \in [0, \infty)\}, \tag{A.8}$$

where $\varepsilon_1 = \alpha$ corresponds to the point $P \in \Sigma_{loc}$ and $\varepsilon_1 = \frac{1}{\alpha}$ corresponds to the point $Q \in \Sigma_{in}$. The variational equations along γ are

$$\begin{pmatrix} \delta a' \\ \delta\rho' \\ \delta\varepsilon' \end{pmatrix} = \begin{pmatrix} (\varepsilon_1 - 1) & \varepsilon_1^2\mu & 0 \\ 0 & -\varepsilon_1 & 0 \\ -2\varepsilon_1 & 0 & 4\varepsilon_1 \end{pmatrix} \begin{pmatrix} \delta a \\ \delta\rho \\ \delta\varepsilon \end{pmatrix} \tag{A.9}$$

coupled to the equation

$$\varepsilon_1' = 2\varepsilon_1^2 \tag{A.10}$$

for ε_1 along γ. Due to the invariance of the ε_1-axis one tangent vector of $\mathcal{M}$ is $(0,0,1)^T$. We conclude from Lemma A.3 that the tangent vector of $\mathcal{M} \cap \Sigma_{loc}$ at the point $P = (0,0,\alpha)$ is $t_P = (\mu\alpha^2, 1, 0)^T$. Note that the first two equations in (A.9) decouple from the third one. By solving the initial value problem

$$\delta a(\alpha) = \mu\alpha^2, \qquad \delta\rho(\alpha) = 1, \qquad \delta\varepsilon(\alpha) = 0$$

for (A.9) coupled to the equation (A.10) for $\varepsilon_1 \in [\alpha, \frac{1}{\alpha}]$ we obtain

$$(\delta a, \delta\rho, \delta\varepsilon)(\varepsilon_1) \approx (\sqrt{\varepsilon_1}, \tfrac{1}{\sqrt{\varepsilon_1}}, *),$$

where the third component $*$ is of no importance since $(0,0,1)^T$ is also tangent to $\mathcal{M}$. Evaluating this expression at $\varepsilon_1 = 1/\alpha$ finishes the proof of the lemma. $\square$

Analysis of π_3. We now switch to chart $\mathcal{K}_2$ to study the transition map $\pi_3 : \Sigma_{in} \to \Sigma_5$ close to the hyperbolic equilibrium p_h from Lemma A.2.

We rewrite system (A.7) as

$$\begin{aligned} a' &= -aF(a,r,\rho) + r(\mu\rho - a - a\rho^2), \\ r' &= -2rF(a,r,\rho), \\ \rho' &= \rho F(a,r,\rho), \end{aligned} \tag{A.11}$$

where $F(a,r,\rho) = 1 - a - a\rho^2$ and the subscript $_2$ of the variables is suppressed. In a small neighborhood of the origin the factor F does not vanish. Hence, we transform (A.11) by dividing out F to obtain

$$a' = -a + \frac{r(\mu\rho - a - a\rho^2)}{1 - a - a\rho^2}, \tag{A.12a}$$

$$r' = -2r, \tag{A.12b}$$

$$\rho' = \rho, \tag{A.12c}$$

The origin is a hyperbolic equilibrium whose eigenvalues are $-1, -2, 1$. It is easy to see that all orbits starting in Σ_{in} with $\rho > 0$ exit through Σ_5. Hence, the map π_3 is well defined and can be approximately described by the linearization. However, the eigenvalues are in resonance ($-1 = -2 + 1$), which indicates difficulties in finding a differentiable coordinate change that linearizes the vector field. Within the invariant plane $\rho = 0$ the eigenvalues are -1 and -2 therefore (A.12) can be linearized in the plane $\rho = 0$ by a smooth near identity transformation

$$a \to \Psi(\tilde{a}, r) \tag{A.13}$$

with $\Psi = \tilde{a} + h(\tilde{a}, r)$, see [23]. A computation shows that $h(\tilde{a}, r) = \frac{1}{2}\tilde{a}r + O(3)$. Under the transformation (A.13) system (A.12) becomes

$$\tilde{a}' = -\tilde{a} + r\rho(\mu + H), \tag{A.14a}$$

$$r' = -2r, \tag{A.14b}$$

$$\rho' = \rho, \tag{A.14c}$$

where $H = H(\tilde{a}, r, \rho) = \tilde{a}h_1 + rh_2 + \tilde{a}\rho h_3$ with bounded smooth functions h_1, h_2, h_3. After these preliminary transformations we prove the following result.

Lemma A.5. *For δ and α sufficiently small the transition map $\pi_3 : \Sigma_{in} \to \Sigma_5$ for system (A.7) is a C^1- map and has the form*

$$\pi_3(a_{in}, \alpha, \rho_{in}) = \begin{pmatrix} \tilde{\pi}_3(a_{in}, \rho_{in}) \\ \alpha(\frac{\rho_{in}}{\delta})^2 \\ \delta \end{pmatrix} \tag{A.15}$$

with $\tilde{\pi}_3(a_{in}, \rho_{in})$ given by

$$\tilde{\pi}_3(a_{in}, \rho_{in}) = \frac{\rho_{in} a_{in}}{\delta} - \mu\rho_{in}^2 \ln \rho_{in} + O(\rho_{in}^2).$$

Proof. In the proof we use system (A.14) to construct the map π_3. The transition time T needed for a point $(a_{in}, \alpha, \rho_{in}) \in \Sigma_{in}$ to reach Σ_5 under the flow of (A.14) satisfies

$$T = \ln(\frac{\delta}{\rho_{in}}). \tag{A.16}$$

We compute (ρ_{out}, a_{out}) as a function of $(\rho_{in}, a_{in}) \in \Sigma_{in}$. Substituting exact solutions of (A.14b) and (A.14c) into (A.14a) we obtain

$$\tilde{a}' = -\tilde{a} + \mu\alpha\rho_{in}e^{-t} + G, \tag{A.17}$$

where

$$G = \alpha\rho_{in}e^{-t}H(\alpha e^{-2t}, \rho_{in}e^t, \tilde{a}).$$

The above equation (A.17) is viewed as a small perturbation of

$$\tilde{a}_0' = -\tilde{a}_0 + \mu\alpha\rho_{in}e^{-t}. \tag{A.18}$$

Equation (A.18) can be solved explicitly,

$$\tilde{a}_0(t) = a_{in}e^{-t} + \mu\alpha\rho_{in}te^{-t}.$$

Suppose the solution of (A.17) has the form

$$\tilde{a}(t) = a_{in}e^{-t} + \mu\alpha\rho_{in}te^{-t} + e^{-t}z, \tag{A.19}$$

where $z(0) = 0$. One gets the following equation for z

$$\begin{aligned} z'(t) = {} & \alpha\rho_{in}[(a_{in}e^{-t} + \mu\alpha\rho_{in}te^{-t})h_1 + \alpha e^{-2t}h_2 + (a_{in}\rho_{in} + \mu\alpha\rho_{in}^2 t)h_3] + \\ & +[\alpha\rho_{in}e^{-t}h_1 + \alpha\rho_{in}^2 h_3]z. \end{aligned} \tag{A.20}$$

We transform the equation (A.20) to the equivalent integral equation of the form

$$\begin{aligned} z(T) = {} & \alpha\rho_{in}a_{in}\int_0^T e^{-t}h_1\,dt + \mu\delta^2\rho_{in}^2\int_0^T te^{-t}h_1\,dt + \alpha^2\rho_{in}\int_0^T e^{-2t}h_2\,dt + \\ & + a_{in}\alpha\rho_{in}^2\int_0^T h_3\,dt + \mu\rho_{in}^3\alpha^2\int_0^T th_3\,dt + \alpha\rho_{in}\int_0^T e^{-t}h_1 z\,dt + \alpha\rho_{in}^2\int_0^T h_3 z\,dt. \end{aligned} \tag{A.21}$$

The bounds for the functions h_i, $i = 1, \ldots, 3$ and $T = \ln\frac{\delta}{\rho_{in}}$ imply that the sum of the first five terms is of order $O(\rho_{in})$. Thus, we have

$$|z(T)| \le O(\rho_{in}) + \alpha\rho_{in}K\int_0^T |z|dt \tag{A.22}$$

with a suitable constant $K > O$. Applying Gronwall's inequality to (A.22) yields to the following result

$$z = O(\rho_{in}).$$

Hence, we obtain

$$\tilde{a}(T) = \frac{\rho_{in}a_{in}}{\delta} - \frac{\mu\alpha\rho_{in}^2}{\delta}\ln(\frac{\rho_{in}}{\delta}) + O(\rho_{in}^2). \tag{A.23}$$

Finally, due to the corresponding inverse transformation $\tilde{a} = \tilde{\Psi}(a, r) = a + O(ar)$, the transition map is given by

$$\tilde{\pi}_3(a_{in}, \rho_{in}) = \frac{\rho_{in} a_{in}}{\delta} - \mu \rho_{in}^2 \ln \rho_{in} + O(\rho_{in}^2)$$

which implies the lemma. □

Proof of Theorem 4.4. Lemma A.3, Lemma A.4 and Lemma A.5 imply all assertions of Theorem 4.4 except the tangency of the curve σ_5 with the line $r_2 = 0$.

In chart $\mathcal{K}_2$ the point Q is given by $(0, \alpha, 0)$ and the tangent vector t_Q of $\mathcal{M}$ is given by $(\sqrt{\alpha}, 0, \frac{1}{\sqrt{\alpha}})^T$. By taking t_Q as a first order approximation of the curve $\mathcal{M} \cap \Sigma_{in}$ and applying the transition map A.15 we obtain that σ_5 is tangent to $r_2 = 0$. □

Max Planck Institute for Mathematics in the Sciences, Inselstrasse 22, D-04103 Leipzig, Germany

E-mail address, I. Gucwa: ilona.gucwa@mis.mpg.de

Institute for Analysis and Scientific Computing, Vienna University of Technology, Wiedner Hauptstrasse 8-10, A-1040 Wien, Austria

E-mail address, P. Szmolyan: szmolyan@tuwien.ac.at

URL, P. Szmolyan: http://www.asc.tuwien.ac.at/szmolyan